Synergistic Effect of Quercetin Magnetite Nanoparticles and Targeted Radiotherapy in Treatment of Breast Cancer

Breast Cancer: Basic and Clinical Research
Volume 16: 1–17

DOI: 10.1177/11782234221086728

Mostafa A Askar[1], Heba AS El-Nashar[2], Mahmood A Al-Azzawi[3], Sahar S Abdel Rahman[4] and Omama E Elshawi[5]

[1]Department of Radiation Biology, National Centre for Radiation Research and Technology (NCRRT), Atomic Energy Authority, Cairo, Egypt. [2]Department of Pharmacognosy and Center of Drug Discovery Research and Development, Faculty of Pharmacy, Ain Shams University, Cairo, Egypt. [3]Department of Pathological Analysis Techniques, College of Medical & Health Technologies, Ahl Al Bayt University, Karbala, Iraq. [4]Department of Pathology, Faculty of Veterinary Medicine, Cairo University, Cairo, Egypt. [5]Department of Health and Radiation Research, National Centre for Radiation Research and Technology (NCRRT), Atomic Energy Authority, Cairo, Egypt.

ABSTRACT: Quercetin is a potent cancer therapeutic agent present in fruits and vegetables. The pharmaceutical uses of quercetin are limited due to many problems associated with low solubility, bioavailability, permeability, and instability. In addition, the high doses of quercetin show toxic effects in clinical and experimental studies. Therefore, a new strategy is warranted to overcome these problems without the use of toxic doses. The iron oxide nanoparticles can be used as a drug delivery system. This study aimed to prepare quercetin-conjugated magnetite nanoparticles (QMNPs) using biological simple nanoprecipitation and mediated by fungus *Aspergillus oryzae*. Also, we initiated in vitro and in vivo studies to determine whether QMNPs might sensitize breast cancer to radiotherapy treatment. The structural, morphological, and magnetic properties of the prepared nanoparticles were studied. The results indicated that QMNPs were spherical in shape and 40 nm in diameter. The in vitro studies showed that the incubation of MCF-7, HePG-2, and A459 cancer cells with QMNPs for 24 h effectively inhibited the growth of cancer cell lines in a concentration-dependent manner with IC50 values of 11, 77.5, and104 nmol/mL, respectively. The combination of QMNPs with irradiation (IR) potently blocked MCF-7 cancer cell proliferation and showed significant changes in the morphology of these cells as observed by bright-field inverted light microscopy. Focusing on the long-term toxicity of QMNPs (20 ml/kg), the assessment of hematological, hepatic, and renal markers indicated no toxic effect. Besides, QMNPs inhibited tumor growth and potently enhanced the lateral radiotherapy treatment in N-methyl-N-nitrosourea (MNU)-induced breast cancer in female white albino rats. These anticancer and radiosensitizing activities were ascribed to cytotoxicity, cell cycle arrest, immunomodulation, and efficiency through induction of apoptosis. In a conclusion, these observations suggest that the QMNPs combined with LRT could act as a potential targeted therapy in breast cancer.

KEYWORDS: Nanoparticles, quercetin, magnetic oxide, apoptosis, radiotherapy, methyl-N-nitrosourea, breast cancer

RECEIVED: November 15, 2021. **ACCEPTED:** February 17, 2022.

TYPE: Original Research

FUNDING: The author(s) received no financial support for the research, authorship, and/or publication of this article.

DECLARATION OF CONFLICTING INTERESTS: The author(s) declared no potential conflicts of interest with respect to the research, authorship, and/or publication of this article.

CORRESPONDING AUTHORS: Mostafa A Askar, Department of Radiation Biology, National Centre for Radiation Research and Technology (NCRRT), Atomic Energy Authority, Cairo, Egypt. Email: mostafa_asker2@yahoo.co; Mostafa.Askar@eaea.org.eg

Heba AS El-Nashar, Department of Pharmacognosy and Center of Drug Discovery Research and Development, Faculty of Pharmacy, Ain Shams University, Cairo, Egypt. Email: heba_pharma@pharma.asu.edu.eg

Introduction

Breast cancer is one of the most common causes of prevalent malignant tumors with an increased mortality rate in the last 5 years.[1] According to statistics of the International Agency for Research on Cancer (IARC) of the World Health Organization (WHO), a total of 18 989 634 new cases of breast cancer associated with 10 052 507 deaths have been developed in 2020 worldwide.[2] Radiotherapy (RT) is one of the commonly used in cancer treatment either alone or in conjunction with surgery and/or chemotherapy. Irradiation kills cancer cells by inducing DNA damage and the generation of reactive oxygen species (ROS).[3] The accumulation of ROS can deregulate the apoptotic signaling pathway, ultimately inducing apoptosis. However, when using external-beam radiation healthy tissues are unavoidably exposed, which increases the probability of normal tissue complication.[4] Reports of the literature evidenced that the use of radiosensitizing agents is one of the ways to enhance RT treatment outcomes and caused better survival in patients with breast cancer.[5] As most radiosensitizers can upregulate ROS which is considered as a potential target to improve RT treatment.[6] It is well known that naturally occurring dietary compounds can fight against the aggressiveness of breast cancer, inhibit cancer cell proliferation, and modulate cancer-related pathways.[7,8] One of these compounds is quercetin (3,5,7,3′,4′-pentahydroxy flavone), a potent cancer therapeutic agent and dietary antioxidant present in fruit and vegetables.[9] Quercetin has selective anti-proliferative and antitumor effects via induction of apoptosis in different human cancer cell lines. Furthermore, it caused cell cycle arrest during G0/G1 in leukemia, S-phase in colorectal carcinoma, and G2/M phases of the cell cycle in leukemia, breast carcinoma, as well as esophageal adenocarcinoma cells.[10] On

the molecular level, it can modulate a number of key targets in cellular signal transduction pathways related to apoptosis such as downregulation of anti-apoptotic proteins of the Bcl-2 family (Bcl-XL and Bcl-2) and up-regulation of pro-apoptotic members (Bax and Bad). Also, it has been demonstrated that quercetin induces apoptosis through a caspase-3-dependent mechanism.[11] It is well known that the interplay between immune cells and tumor cells exerts a major influence on breast tumor development and progression,[12] and the development of cancer is associated with alterations in numbers and functions of immune cells in the peripheral circulation and especially at the sites of tumor progression.[13] Quercetin showed antitumor activity via stimulation of the immune system.[14] T-Cells (1 of the 2 main arms of the acquired immune system) comprise one of the major components of the adaptive immune response. There are 2 antagonistic classes of T-cells that have an important role in fighting against cancer cytotoxic CD^{8+} T-cells and CD^{4+} regulatory T-cells (Tregs). Cytotoxic CD^{8+} T-cells are essential for the direct killing of cancer cells. Tregs are immunosuppressive cells with a central role in maintaining self-tolerance and immune homeostasis.[15] According to the literature, studies reporting potential synergistic effects when combined with quercetin with RT can enhance tumor radiosensitivity both *in vitro* and *in vivo*. Quercetin can also protect normal cells from the side effects caused by RT, which obviously provides notable advantages in their use in anticancer treatment.[16] Despite its numerous biological effects, the pharmaceutical use of quercetin is limited due to some challenges such as low solubility, bioavailability, permeability, and instability. Furthermore, enzyme digestion of quercetin in the digestive tract is overrated, and its survival time in blood circulation is low.[17] The formulation of quercetin nanostructures has been conducted to increase its solubility and bioavailability,[18] and thereby improve their target specificity to cancer cells or tumors by lowering the toxicity or side-effects to normal cells.[19] In this regard, magnetic nanoparticles comprise important characteristics that make them attractive for a variety of biomedical applications. Specifically, iron oxide magnetic nanoparticles (IONPs) are physically and chemically stable, biocompatible, and environmentally safe.[20] Owing to their cost benefits and the harmful effects to the environment, the chemical and physical methods for the synthesis of nanoparticles are limited. So, biosynthesis is, therefore, the best choice because it stands out as a simple, low-cost, and ecofriendly route for IONPs production.[21] In this method, the biological system with its reducing potential can interact with iron to transform the organic metal into metal nanoparticles via the reactive capacity of proteins and metabolites present in these organisms.[22] In the present research, quercetin-loaded magnetic NPs were biologically synthesized and mediated by *A. oryzae* for the first time using $FeSO_4$ as a substrate to yield magnetite (Fe_3O_4) NPs. So, this study was conducted to characterize the synthesized quercetin magnetite nanoparticles (QMNPs). We also aimed to provide sufficient evidence about the safety or toxicity (acute and long-term) of the synthesized QMNPs on the cellular level in treated rats as compared with the control rats in the range of the applied dose during the study. The toxicity evaluation was done via investigation of hematological and biochemical parameters such as hepatic and renal biomarkers. Furthermore, the cytotoxicity and antitumor activity of QMNPs and their efficacy to enhance the radiosensitivity of breast cancer cells was demonstrated *in vitro* and *in vivo* with a focus on assessment of the underlying critical mechanism.

Materials and Methods

1-methyl-1-nitrosourea (MNU) and Quercetin (Q4951), KH_2PO_4; K_2HPO_4; $MgSO_4$; $(NH_4)_2SO_4$; $K_4Fe(CN)_6$, and $FeSO_4$ were (Sigma Aldrich). HePG2, MCF-7, and A-549 cancer cell lines were purchased from the tissue culture unit of the Holding Company for Biological Products and Vaccines (VACSERA), Giza, Egypt, and supplied through the American Type Culture Collection (ATCC). All cell culture material was obtained from Cambrex BioScience (Copenhagen, Denmark). *A. oryzae* fungus was kindly provided by the culture collection unit of the Regional Center for Mycology and Biotechnology (RCMB) Al-Azhar University, Cairo-Egypt. The fungal isolate was subcultured and maintained on Sabouraud's Glucose agar (SGA) medium containing; 20 g/L glucose; 10 g/L peptone–; 20 g/L agar–and 1000 mL distilled water, at the temperature of 25 (±2)°C and the pH was adjusted at 5.4 ± 0.2.

Preparation of QMNPs

The biomass of the fungal extract was prepared according to the previously described method,[23] with some modifications. The fungus was grown aerobically in a liquid medium containing: 7 g/L; 2.0 KH_2PO_4; 0.1 g/L $MgSO_4$; 1 g/L $(NH_4)_2SO_4$; 0.6 g/L yeast extract; and 10 g/L glucose–10.0 at pH (6.2 ± 0.2). The flasks were inoculated and incubated on an orbital shaker at 25°C and agitated at a speed of 150 r/min. The biomass was harvested after 72 h of growth by sieving through Whatman filter article no.1 followed by extensive washing with distilled water to remove any component from the biomass. In this work, FeSO4 was used as a substrate to prepare QMNPs and mediated biologically by *A. oryzae.* At first, the extracellular bio extract of the fungal was prepared for the biosynthesis of Fe3O4. For this purpose, 20 g of fresh clean fungal biomass was brought in contact with 100 mL of deionized water in an Erlenmeyer flask and incubated at 25°C in a dark shaking incubator (150 r/min) for 72 h. After the incubation period, the cells filtrate was obtained by passing it through Whatman filter article no.1. Second, for the synthesis of the MNPs by using FeSO4 as a substrate, 100 mL of cell-free water extract of *A. oryzae* were exposed to 10 mM $FeSO_4$ aqueous solutions at (pH 3.1) in 500 mL Erlenmeyer flasks and kept on a shaker (200 r/min) at 27°C. The reaction was carried out for a period of 120 h in place of the iron cyanide complexes of the earlier experiment. All of the bio-transformed nano-products were

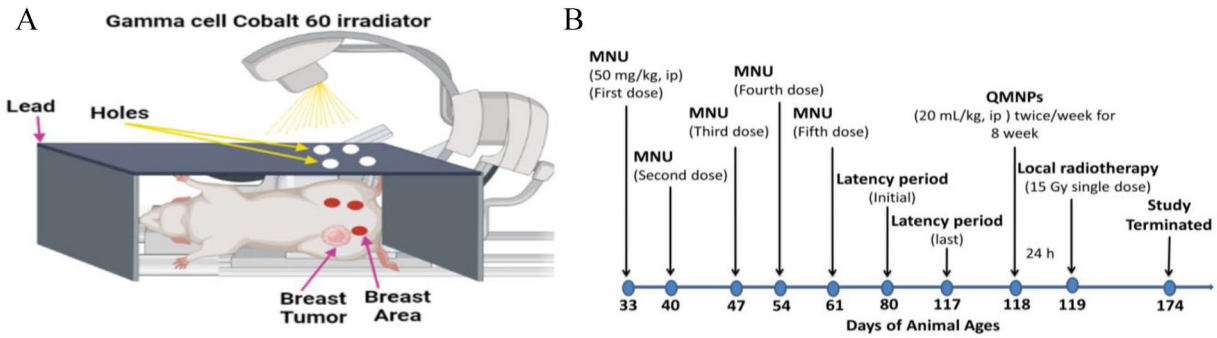

Figure 1. (A) Diagram of animal local RT by cobalt 60 and (B) schematic illustration of the experimental design and tumor induction. MNU indicates 1-methyl-1-nitrosourea; QMNP, quercetin magnetite nanoparticles.

centrifuged at 10 000 r/min for 15 min, following which the pellet was re-dispersed in sterile distilled water to dispose of any uncoordinated biological molecules. The process of centrifugation and re-dispersion was run in sterile distilled water and repeated 3 times to ensure better separation of free entities from the metal nanoparticles. The purified pellets were then sonicated for 30 min using an ultrasonicator (united Jeveriy tools supplies, Italy) for more disparity. Finally, samples were freeze-dried using a lyophilizer (Thermo Electron Corporation, Micro Modulyo 230 freeze dryer). The lyophilized powder was ready for further analysis and characterization.

Characterization of QMNPs

Characterization of the prepared MNPs and QMNPs was carried out by different instruments and techniques. It includes visual observation; UV-Visible spectrophotometer, transmission electron microscope (TEM), X-ray diffraction (XRD), and Fourier transform infrared (FTIR) analysis.

Gamma-ray irradiation

MCF-7 cells were treated with a single-dose 6 Gy γ-radiation,[24] using a cesium-137 source (Gammacell 40 Exactor; NCRRT, AEA, Cairo, Egypt). The dose rate used was 0.423 Gy/min. The dosimetry was used for all experiments to ensure uniformity of dose and dose rate delivered using the Fricke reference standard dosimeter.[25] Local RT of the tumors was started when tumors were detected and reached ~5 to 7 mm^2 in size at 119 days of animal age. Mice were anesthetized with an intraperitoneal (*i.p.*) injection of Phenobarbital 50 mg/kg and positioned in a Lucite jig with lead shielding the body and only the breast bearing the tumor exposed for radiation treatment in the Gamma cell Cobalt 60 irradiator at the cancer treatment unit, National Center for Radiation Research and Technology (NCRRT), Atomic Energy Authority (AEA) Cairo, Egypt.[26] Rats received a single local dose of 15 Gy,[27] on 119 days of animal age, using a Cobalt 60 source operating using a 250 kV orthovoltage system at a dose rate of 205/69c Gy/min with a distance of 7.5 cm on the field of 35 × 35 in the dorsoventral axis. A custom-designed positioning device based on the standard stereotactic frame was used so that 10 animals could be simultaneously irradiated (Figure 1A). The dosimetry was performed by implanting lithium fluoride thermoluminescent dosimeters into various areas. Each 10 rat was confined to sit under led plate with its tumor-bearing breast extended through an opening in the side of the breast to allow the tumor site to be irradiated locally.

In vitro study

Cytotoxicity assay. Cellular toxicity was run according to Foo et al[28] using 3-(4, 5-dimethylthiazol-2-yl)-2,5-diphenyl tetrazolium bromide (MTT) to demonstrate the cytotoxic potential of the engineered QMNPs on the viability of the human cancer cells (HePG2, MCF-7, and A-549). The cells were plated separately in 96-well plates at a concentration of 5 × 105 cells/well. After 24 h, cells were washed twice with 100 µL of serum-free medium and starved for 1 h at 37°C. After starvation, cells were treated with 20 µL of serial concentrations of the tested material for 48 h at 37°C, in a humidified 5% CO_2 atmosphere. After incubation, media were removed and 40 µL MTT solution/well was added and incubated for an additional 4 h. The absorbance of the purple-blue formazan dye was measured spectrophotometrically in a microplate ELISA reader (ELx808 Absorbance Reader) at 570 nm. The experiment was carried out in triplicates, and the average of the viable cells was calculated. A graph was plotted between the percentage of the viable cells and dilution. Data were expressed as the percentage of relative viability compared with the vehicle control.

Estimation of the optimal irradiation dose and radiosensitizing effect of QMNPs. MCF-7 cells were used for the determination of the optimal irradiation dose that causes inhibition of proliferation. The cell lines were exposed to 0, 4, 6, 8, and 10 Gy. Briefly, 103 to 10^5 cells/well were loaded in a 96-well plate, thereafter; the cells were maintained in 5% CO_2 at 37°C for 24 h. Cells were incubated in MTT (5 mg/mL) for 4 h at 37°C and measured at 570 to 630 nm in an ELISA reader *(ELx808 Absorbance Reader*) with the solubilization buffer as blank. Percentage of cell viability was determined according to the following formula:

$$\% \text{ of cell viability} = \left[\frac{OD_{570\text{-}630} \text{ of the treated cells}}{OD_{570\text{-}630} \text{ of the untreated control}} \right]$$

In the subsequent study, the radiosensitizing effect of QMNPs by the culture medium of the control set remained without any treatment. For the other treatments, the culture media were removed and replaced with the QMNPs at a concentration of 11 nM/mL (IC50) for the sole drug treatment, another 2 sets were exposed to 6 Gy (optimum dose) either alone or in combination with QMNPs (11 nM/ml QMNPs + 6 Gy irradiation). All the experiments were incubated for 24 h, thereafter, 20 µL of MTT (5 mg/mL in PBS) was added to each well, and samples were incubated for 4 h at 37°C and measured as above.

In vivo study

The study was approved by the research ethics committee for experimental studies (Human and Animal subjects) at NCRRT, EAEA, (Cairo, Egypt), following the 3Rs principle for animal experimentation (Replace, Reduce, and Refine) and is organized and operated according to Council for International Organizations of Medical Sciences and International Council for Laboratory Animal Science International Guiding Principles for Biomedical Research Involving Animals 2012 (serial number: 4A/20).

LD_{50} and toxicity estimation of QMNPs

Acute and long-term toxicities were performed to provide information on the possible health hazards likely to arise from single or multiple exposures to QMNPs after *i.p.* injection within a period of 3 days (acute toxicity) and 8 weeks (long-term toxicity). For acute toxicity, 5 groups of animals (n = 6/group) of animal weight average of 120 ± 5 gm were used. Different concentrations (1, 10, 20, 40, and 80) mL/kg of QMNPs were delivered to the animals. The rats were observed daily for any signs of toxicity, morbidity, and mortality for 72 h. The long-term toxicity of QMNPs was evaluated in the range of the dose used in the *in vivo* studies (20 mL/kg body weight, twice/week for 8 weeks) using the control group (n = 10) and rats treated with QMNPs (n = 10). These animals were observed for 8 weeks for the evidence of any adverse toxicity or death following QMNPs treatment. At the end of the experimental period, blood was collected from the carotid artery. Blood was separated into 2 parts: (1) with an anticoagulant agent to examine complete blood count and (2) plasma was separated to examine the biochemical effect of the QMNPs (20 mL/kg).

Experimental design and tumor induction

Female Wistar Albino rats (n = 90) injected *i.p.* with MNU (50 mg/kg) dissolved freshly in 0.9% NaCl and adjusted to pH = 4.0 with acetic acid for activation. The injection of the carcinogen was at 33, 40, 47, 54, and 61 days of the animal's age according to the previous method.[29] The animals were weighed weekly and palpated to record the numbers, location, and size of tumors.

Female Sprague–Dawley rats (n = 90) aged 45 to 50 days were randomly categorized into 2 main groups (Figure 1B): group I (n = 10 rats): which served as the control, and group II (n = 80), injected *i.p.* with MNU (50 mg/kg) dissolved freshly in 0.9% NaCl and adjusted to pH = 4.0 with acetic acid for activation. The injection of the carcinogen was at 33, 40, 47, 54, and 61 days of the animal's age. The animals were weighed weekly and palpated to record the numbers, location, and size of tumors. When tumor size reached 0.5 cm in the largest dimension (45 rats had this inclusion criterion), group II was randomly divided into 4 groups:

II. Tumor group (n = 15): animals received the vehicle of CUR-NAR-D-MNPs.
III. RT group: tumor-bearing animals were exposed to local RT (15 Gy) once at 119 days of animal age.
IV. QMNPs: tumor-bearing animals have received a dose of 20 mL/kg of QMNPs via *i.p.*, twice per week, which started at 118 days of animal age after the latency period (the last tumor was observed at 117 days) and continued for 8 weeks.
V. QMNPs + RT: tumor-bearing animals were treated with QMNPs, then animals were exposed to RT (15 Gy).

Mortality and body weight gain were recorded weekly. Tumor volumes and weights were calculated using the following formula: $L/2 \times W/2 \times \pi$.[30] At the end of the experimental study at 174 days, the animals were sacrificed; blood was collected, and breast tissues were separated to examine the biochemical and histological changes.

Hematological and biochemical analysis

The hematological indices were demonstrated using the hematology analyzer system (CELL-DYN 1700 (Abbott Diagnostics, Abbott Park, IL, USA). Alanine aminotransferase (ALT) and aspartate aminotransferase (AST) activities,[31] albumin levels (Alb),[32] serum creatinine,[33] and urea.[34] The oxidative status was evaluated via assessment of malondialdehyde (MDA),[35] reduced glutathione (GSH),[36] superoxide dismutase (SOD),[37] and catalase (CAT).[38]

Histopathological examination

The part of breast tissues of control rats and breast cancer masses from the other group were fixed in 10% formol saline for 24 h, washed in tap water, and followed for dehydration by serial dilutions of alcohol (methyl, ethyl, and absolute ethyl).

Samples were embedded in paraffin after being cleared in xylene and at 56 C in a hot air oven for 24 h. By slides microtome, paraffin beeswax tissue blocks were prepared for sectioning at 4 µ thickness. The obtained sections were collected on glass slides, deparaffinized, and stained using hematoxylin and eosin (H&E) for routine light electronic microscope examination.[39]

Enzyme-linked immunosorbent assay

Bcl-2 and caspase-3 levels were determined by using the markers assay kit (MyBioSource; Cat. No: MBS2881713 and MBS841649 respectively), following a modification of the manufacturer´s protocol. 10% tissue homogenate was obtained from the mammary tissue samples in PBS consisting of a 1% protease inhibitor cocktail. Furthermore, the homogenates were undergone centrifugation (12 000 g for 15 min) for about 15 min, and the resulting supernatants attained were collected. Reactions were carried out following the manufacturer's protocol, and absorbance was measured at 450 and 405 nm, respectively using an automatic microplate reader (Quant, BioTek Instruments, Inc.,Winooski, VT, USA).

Flow-cytometry analysis of the cell cycle, CD4+, and CD8+

After 24 h of exposure to 6 Gy and/or RT QMNPs (11 nM/mL) treatment, MCF-7 cells were seeded in 6-well plates at 1.3×10^5 cells in 3 mL of complete growth culture media, incubated for 24 h. Following incubation, the floating cells were collected, and adherent cells were harvested by trypsinization to detach the cells and pelleted at 100*g* for 5 min. Cells were washed twice with PBS and resuspended in 70% ethanol at −20°C overnight. Isolated tissues for all groups were processed immediately. Breast tissues were cut into pieces of 2 to 5 cm thickness, rinsed, and cleaned with PBS. Fresh tissues were mechanically dispersed, sequentially using 100 and 35 µm nylon cell-strainers (mesh) (BD-Falcon:0877119). Specimens were pressed through the 100 µm mesh, which was placed in a tissue culture dish containing PBS/EDTA. The mesh was rinsed several times at 4°C cold PBS/EDTA and centrifuged for cell suspension (310*g*; 4°C; 6 min). The supernatant was removed, and 5 mL cold ethanol (80%, −20°C) was added dropwise under constant, gentle, vortexing to fixed cells. Before staining, cells were kept at −20°C overnight. For the cell cycle analysis, cells were treated with an appropriate volume of staining solution containing 30 µg/mL PBS, and 0.3 mg/mL RNase-free DNase. For the cell surface markers (CD^{4+} and CD^{8+}), cells were stained with a 10µL monoclonal antibody in the dark for 30 min at room temperature. (BD-Pharmingen™, Cat. Nos. (557307 and 746832, respectively). The cell cycle and cell surface marker data were analyzed by BD Accuri-C6-Plus software (Biosciences,CA, USA).[40]

Statistical analysis

All experiments were performed at least in triplicate, and the results were expressed as the mean ± standard error (SEM). The statistical software package (SPSS, 20, Inc., Chicago, IL) was used for analysis. Statistical significance between all groups was analyzed using the $P < 0.001$, $P < 0.01$, and $P < 0.05$. Statistical analyses were performed using Prism, version 7 (GraphPad Software, La Jolla, CA)

Results

QMNPs characterizations

Visual characterization of the synthesized QMNPs showed that the *A. oryzae* cell-free water extract was pale yellow before the addition of iron nanoparticles (Figure 2BA), which changed to a golden brownish color indicating completion of the reaction with $FeSO_4$ after 28 h (Figure 2BB). The later color turned to dark brownish as magnetite (Fe_3O_4)-quercetin forming complex achieved by time (Figure 2BC). The features of the UV-vis spectrum of the synthesized QMNPs are indicated in 2 curves (Figure 2C). Two intensive absorption bands of magnetite were observed in curve 1 centered at 360 nm and 254 nm. In curve 2, 2 absorption peaks of QMNPs were observed at 256 nm and 377 nm. The absorption peak II of curve 2 was shifted 2 and 17 nm, respectively.

The transmission electron microscope image showed that the particles were spherical in shape and uniformly distributed (mono-dispersed) without significant agglomeration. The formulated MNPs were ~11 nm in diameter (Figure 2DA), meanwhile, QMNPs were spherical in shape and 40 nm in diameter (Figure 2DB). The XRD image (Figure 2E), showed that the Fe_3O_4 NPs were pure magnetite (Fe_3O_4) with a cubic inverse spinel structure. The diffraction peaks belong to Fe_3O_4 NPs prepare by $FeSO_4$ substrate were (111); (220); (311); (400); (422); (511); (440), (533); (553). The diffraction peaks belong to QMNPs prepared by $FeSO_4$ substrate were (220); (311); (400); (422); (511); (440). Iron, as well as quercetin-iron complex nanoparticle characteristic peaks by the FTIR, were shown in (Figure 2F), there was a strong absorption peak at 1654 cm^{-1} to quercetin for C-O telescopic vibration of carbonyl C-4. The vibration frequency of quercetin (C–O) and Fe ion formation complexes was shifted to 1635 cm^{-1}, moved a low wavenumber 19 cm^{-1}. It could be inferred quercetin 4 C–O participates in the match. At 623 cm^{-1} it appeared in ν (M–0) for complexes that could be inferred metal coordination bond formation. There was a smaller change for the ν (C–O–C) compared between quercetin and Fe ion formation complexes but also showed the oxygen of C-ring did not happen with the role of metal ions. In 3404 cm^{-1} absorption peaks, nano magnetite (Fe_3O_4) might through the surface adsorption effected on complexes, may also through its surface hydroxyl and complexes formed the hydroxyl, or magnetite (Fe_3O_4) nanometer

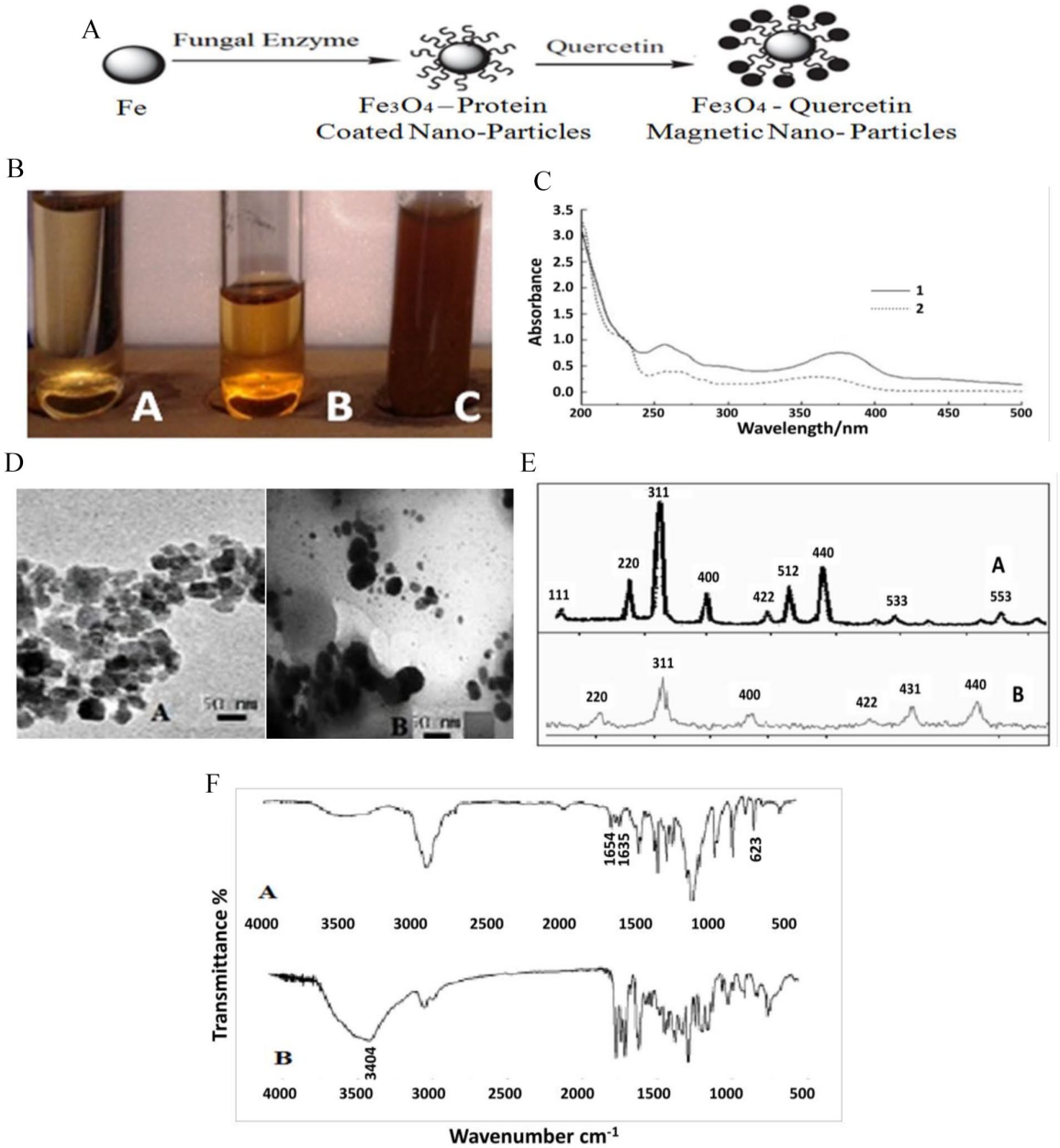

Figure 2. Structural preparation and characterization of QMNPs: (A) schematic illustration of the reaction mechanisms for the overall synthesis process of the quercetin-loaded Fe3O4 nanoparticles via *A. oryzae*, (B) visual characterization of the synthesized QMNPs, (C) the chromatogram of UV spectrophotometry of MNPs (curve 1) and QMNPs (curve 2) mediated by *A. oryzae* using FeSO4 as a substrate, (D) TEM images of the synthesized MNPs (A) and QMNPs (B) mediated by *A. oryzae* and FeSO4 as a substrate, magnification ($X = 200\,000$ K for A and $X = 100\,000$ K for B). (E) XRD patterns of the synthesized MNPs (A) and QMNPs (B) mediated by *A. orrzae* and FeSO4 as a substrate. (F) FTIR analysis of magnetite (Fe3O4) nanoparticles (A), magnetite (Fe3O4)–quercetin with FeSO4 substrate.
FTIR indicates Fourier transform infrared; MNP, magnetite nanoparticles; QMNP, quercetin magnetite nanoparticles; TEM, transmission electron microscope; UV, ultraviolet; XRD, X-ray diffraction.

hydrogen and complexes formed a metal bond. But it was considered that nano magnetite (Fe_3O_4) was insoluble in ethyl alcohol, so it was regarded as which was formed cladding by nano magnetite (Fe_3O_4) and quercetin-Fe metal complexes.

Cytotoxicity and IC_{50} of QMNPs

The cytotoxicity of the QMNPs and IC_{50} values was evaluated against the viability of HePG-2, MCF-7, and A459 cancer cells (Figure 3A). The cells were treated with different concentrations ranging from 5 to 40 nmol/mL in comparison with untreated control cell lines. The results showed that MCF-7 cells appeared to be more sensitive with the IC_{50} value of 11 nM/ml. Meanwhile, the IC_{50} values were found to be 40 and 37.5 nmol/mL for HePG-2 and A459 cell lines, respectively. The results also, clearly suggest that QMNPs exhibited cell specificity and concentration-dependent cytotoxicity. Taking into account these data, the MCF-7 cell lines and

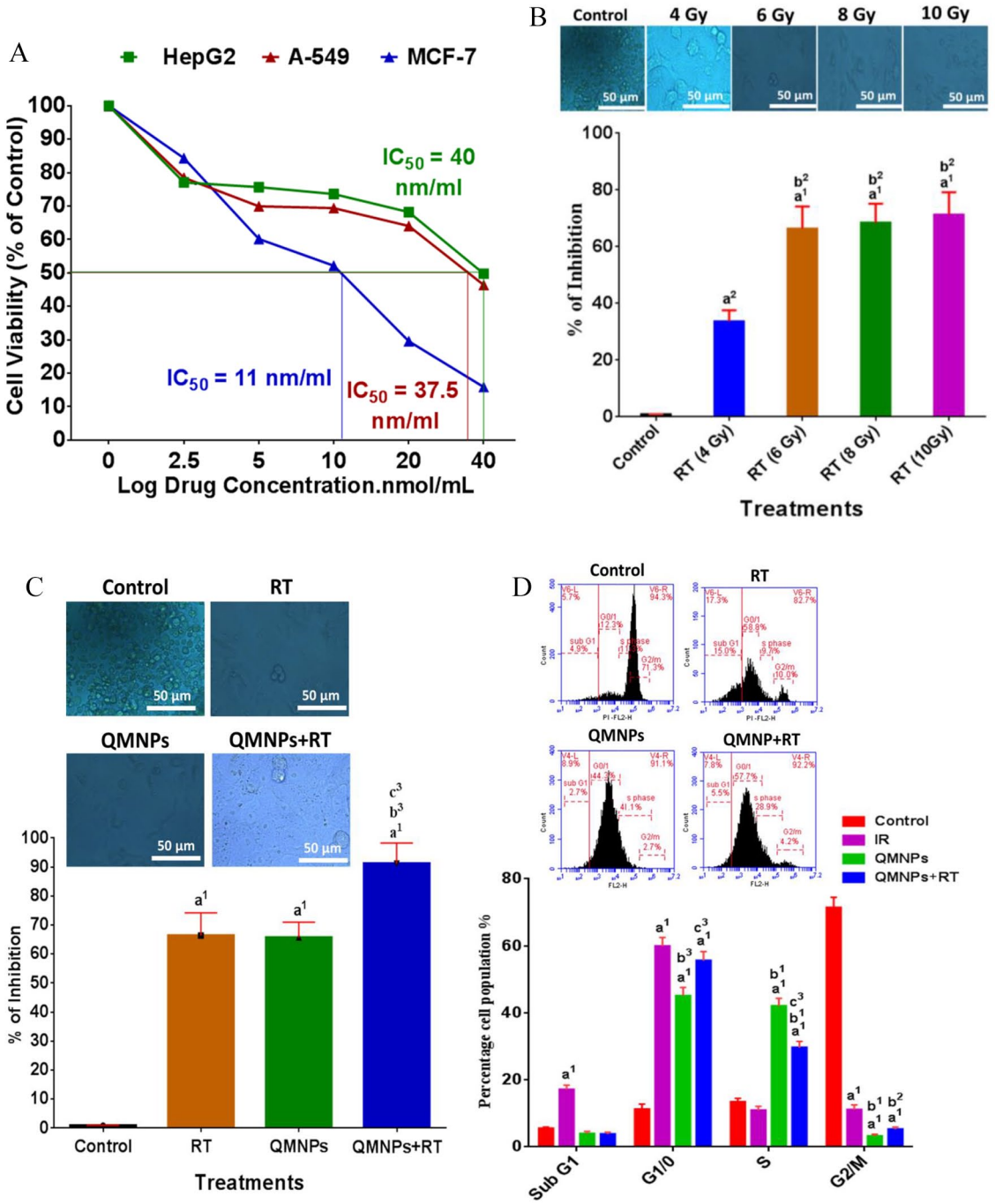

Figure 3. (A) Dose-dependent cytotoxicity and IC50 values of QMNPs on MCF-7, Hep-G2, and A-549 cell lines at 24 h treatment. (B) Estimation of the optimal radiotherapy dose on MCF-7 cell line. (C) Radiosensitization effect of QMNPs on MCF-7 cell line using; MCF-7 cells treated with 11 nmol/mL QMNPs for 24 h prior to exposure to 6 Gy γ-ray. (D) Effect of QMNPs and/or RT on cell cycle distribution. Values expressed as the mean ± SEM, n = 5. QMNP indicates quercetin magnetite nanoparticles; RT, radiotherapy; SEM, mean ± standard error.
$^{a1}P < .001$, $^{a2}P < .01$ vs control; $^{b1}P < .001$, $^{b2}P < .01$, $^{b3}P < .05$ vs RT group (4 Gy) and RT (6 Gy); $^{c3}P < .05$ vs QMNPs group.

concentration of QMNPs (11 nmol/mL) were used for the subsequent *in vitro* studies.

Estimation of the optimal irradiation dose

The MCF-7 cell lines were exposed to different doses of radiation to demonstrate the optimal radiation dose using MTT assay. Photographs using a bright-field inverted light microscope (Figure 3B) demonstrated that MCF-7 cell lines of the control cells appeared round meanwhile displaying variable degrees of reduction in cell viability accompanied with morphological changes after exposure to 4, 6, 8, and 10 Gy, respectively. The pronounced reduction and the greater morphological changes which were closely correlated with reduction of the viable cells were shown in 6 Gy-exposed cells than that of the other sets. Thus, the 6 Gy dose was chosen which was used for *in vitro* further investigations.

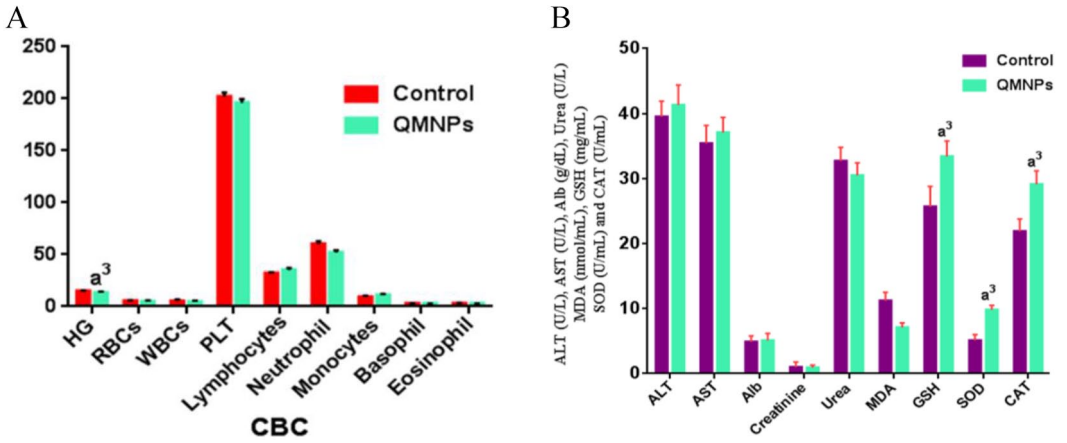

Figure 4. QMNPs effect on vital indices: (A) hematological indices, (B) hepatic, renal markers, and antioxidants/oxidative markers. Values expressed as the mean ± SEM, n = 5.
ALB indicates albumin; ALT, alanine aminotransferase; AST, aspartate aminotransferase; CAT, catalase; GSH, glutathione; MDA, malondialdehyde; PLT indicates platelets; QMNP, quercetin magnetite nanoparticles; RBC, red blood cells; SEM, mean ± standard error; SOD, superoxide dismutase; WBC, white blood cells.
$^{a3}P < .05$ vs control.

The radiosensitization effect of QMNPs

In this study, the MTT assay was used to determine the enhancing killing effect of radiation dose to MCF-7 by QMNPs (Figure 3C). The dead cells were 0.9 ± 0.1 in the control set. These values were increased to 66.4 ± 7.8 and 65.7 ± 5.3 after the single treatments of RT (6 Gy) and QMNPs (11 nmol/mL), respectively, compared with the control set. Nevertheless, the dual treatment of QMNPs and RT enhanced the killing effect of the γ-irradiation as indicated by the great reduction of cells survival by 91.2 ± 7.1%, comparable with the survived cells after exposure to RT or QMNPs alone. The morphological changes were synchronized with the killing effect of each treatment used (Figure 3C). The photographs showed that each of the single treatments of radiation and QMNPs caused distinct morphological DNA damage characteristics such as cell shrinkage with intact membranes as well as condensed cytoplasm along with membrane blebbing, which led to the formation of apoptotic bodies. The great pronounced morphological changes were noticed after exposure to the dual treatment.

QMNPs induced G1/S phase cell cycle arrest and enhanced irradiation-mediated G1 phase arrest in vitro

Cell cycle distribution of nuclear DNA in MCF-7 human cancer cell lines in the different examined groups was determined through the PI staining method followed by Flow-cytometry analysis to measure the percentage of distribution of cell fractions in each of the cells cycle phases (Figure 3D). In the control group, the percentages of cells were 5.5 ± 0.4, 11.2 ± 1.6, 13.4 ± 1.1, and 71.4 ± 3.1 that showed the normal pattern of DNA content and reflect sub-G1, G1/G0, S, and G2/M phases of the cell cycle, respectively. Radiotherapy treatment increased the DNA content in the sub-G1 phase (17.1 ± 1.3) and caused G1/G0 phase (55.6 ± 2.7). Quercetin-conjugated magnetite nanoparticles caused G1 phase (45.1 ± 2.5) and S phase (42 ± 2.3) arrest compared with the control group. More and above, QMNPs obviously enhanced the killing effect of RT treatment as the percentage of cells reached 59.9 ± 2.6 in the G1 phase compared with RT-treated cells.

In vivo studies

Acute and long-term toxicity estimation of QMNPs. For 72 h observation, after injection of different concentrations of QMNPs (1, 10, 20, 40, and 80 mL/kg), the animals did not show any abnormal signs and no mortalities. No physical discomfort in the form of tremor, convulsion, salivation, diarrhea, lethargy, sleep, or coma was observed verifying the nontoxic nature of the synthesized nanoparticles even at the high dose, suggesting that LD_{50} value was higher than 80 mL/kg of QMNPs.

In the subsequent *in vivo* studies, the light has been shed also, on the possible long-term toxicity of QMNPs on the cellular level within the range of the dose used during this work (20 mL/kg) given twice weekly for 8 weeks.

A complete blood count (CBC) analysis was done for treated rats and compared with those of the control group. The collected data revealed a significant decrease in hemoglobin (Hb) levels, meanwhile, there were not any significant changes were recorded in the other hematological indexes, compared with those of the control rats (Figure 4A).

Statistically, insignificant change was recorded in hepatic markers (ALT, AST, and Alb), and renal metabolites (creatinine and urea), compared to those of the control rats (Figure 4B).

In the control group, MDA value was 11.2 ± 1.3, GSH level was 5.1 ± 3.1 and 21.9 ± 0.9, SOD and CAT activities were 25.7 ± 1.9, respectively. These recorded a significant decline in MDA level (7.1 ± 0.7) associated with a profound elevation in

Table 1. QMNPs and/or RT effect on mortality, weight, tumor weight, and tumor volume.

GROUPS	PARAMETERS				
	NUMBER OF ANIMALS	MORTALITY (%)	WEIGHT GAIN	TUMOR WEIGHT (GM)	TUMOR VOLUME (MM3)
Control	10	20%	118.0 ± 2.7	–	–
Tumor	20	70%^{a1}	91 ± 2.3^{a1}	41.2 ± 1.3	409 ± 7.3
RT	20	70%^{a1}	97 ± 1.9^{a1}	30.1 ± 2.1^{b3}	326.5 ± 5.5^{b1}
QMNPs	20	60%$^{a1, b3, c3}$	$99 \pm 1.8^{a1, b3}$	31.2 ± 1.1^{b3}	320 ± 6.2^{b1}
QMNPS + RT	20	50%$^{a1, b2, c2, d3}$	$108 \pm 2.5^{a3, b1, c3, d3}$	$20.1 \pm 1.5^{b1, c3, d3}$	$195.3 \pm 5.7^{a1, b2, c2, d3}$

Abbreviations: QMNP, quercetin magnetite nanoparticles; RT, radiotherapy.
The results presented as the mean ± SEM. $^{a1}P < .001$, $^{a3}P < .05$ vs control; $^{b1}P < .001$, $^{b2}P < .01$, $^{b3}P < .05$ vs tumor group; $^{c2}P < .01$, $^{c3}P < .05$ vs RT group, $^{d2}P < .01$, $^{d3}P < .05$ vs QMNPs.

GSH level (9.4 ± 0.4), and SOD ($33. \pm 2.4$) and CAT (29.1 ± 2.1) activities compare to 11.2 ± 1.3 (MDA), 5.1 ± 3.1 (GSH level), 21.9 ± 0.9 (SOD), and 25.7 ± 1.9 (CAT) activities in the control group (Figure 4B).

Effect of QMNPs and/or RT on morphological and histopathological indices. As shown in (Table. 1), 70% of mortalities were noted in animals after MNU injection (*i.p.*), which may be due to MNU-toxicity. The tumor group had a significant decrease in weight gain, compared with the control group. Meanwhile, the rats treated with QMNPs and/or RT had a significantly increased weight gain, compared with the tumor group. Otherwise, the rats treated with QMNPs and/or RT showed significant regression in tumor volume and weight, compared with the tumor group. Moreover, QMNPs significantly enhanced the effect of RT treatment to induce more reduction in tumor volume and tumor weight, compared with the single treatment.

As shown in Figure 5, no morphologic changes were detected in the breast tissue of control rats. While the tumor group showed a large solid mass (masses) with variable sizes of breast cancer. A marked regression in the tumor size was observed after RT treatment or QMNPs treatment. Furthermore, an increase in this regression was shown in the animal group delivered the dual treatment.

The histopathological examination of the mammary gland (Figure 5), confirmed that the control rats have normal mammary acini with normal epithelial linings embedded in the surrounding adipose tissue. While the mammary gland of tumor rats showed well-differentiated adenocarcinoma with various histological subtypes including solid, comedo, cribriform, and comedo-cribriform subtypes and few showed cystic type. All these changes were accompanied by variable degrees of ductal epithelial hyperplasia. The neoplastic cells appeared pleomorphic, and others appeared uniform with basophilic to eosinophilic cytoplasm. They contained centrally or basally located rounded or oval nuclei. The mitotic figures were sometimes exceeded 8/high microscopic field. The solid type is formed from solid rounded or oval masses of neoplastic cells separated by thin fibrous bands. While the cribriform adenocarcinoma appeared as solid masses of tumor contained numerous variable sizes small empty spaces scattered throughout the mass. In the comedo-form, the neoplastic cellular masses appeared with centrally located cellular debris. The massive stromal response was evident and characterized by fibrosis and mononuclear inflammatory cells infiltration with or without variable degrees of hemorrhage. While examination of the mammary gland of γ-irradiated rats showed fulminating necrosis of cancer cells appeared as large eosinophilic granular areas of necrosis among the tumor masses. Some of the later neoplastic cells showed cytoplasmic vacuolation. Regarding the mammary gland treated with QMNPs, the examination revealed marked swelling, vacuolation with nuclear pyknosis, and necrosis of cancer cells with the presence of large cystic fluid-filled spaces in some cases and marked inflammatory reaction as well. The beginning of fibrous bands proliferation among groups of cancer cells was noticed. Regarding examination of mammary gland sections of the treated groups; it was clear that the dual treatments caused the best suppressive effect against the tumor growth over the only QMNPs. Administration of combined QMNPs and RT conspicuously affected the neoplastic cells causing an obvious marked cellular necrosis and transformation of the cancer cells into hyalinized eosinophilic material with many pyknotic nuclei. Some cases showed marked vacuolation, nuclear pyknosis and necrosis of the cancer cells with appearance of eosinophilic derbies, and sometimes fibrous replacement of the cancer masses were noticed to such extent that it was difficult to assure presence of the previous tumor mass.

Effect of QMNPs and/or RT on cell cycle and apoptosis in breast tissue. As shown in (Figure 6A and B), most cells in the control group are blocked in the G0/1 phase before treatments. In addition, the distribution of most cells in the tumor group was concentrated in the G2/M phase with a significant increase in the level of anti-apoptotic Bcl-2, and a significant decrease in the apoptotic caspase-3 level, compared with those of the control group. Furthermore, we found that most cells in the

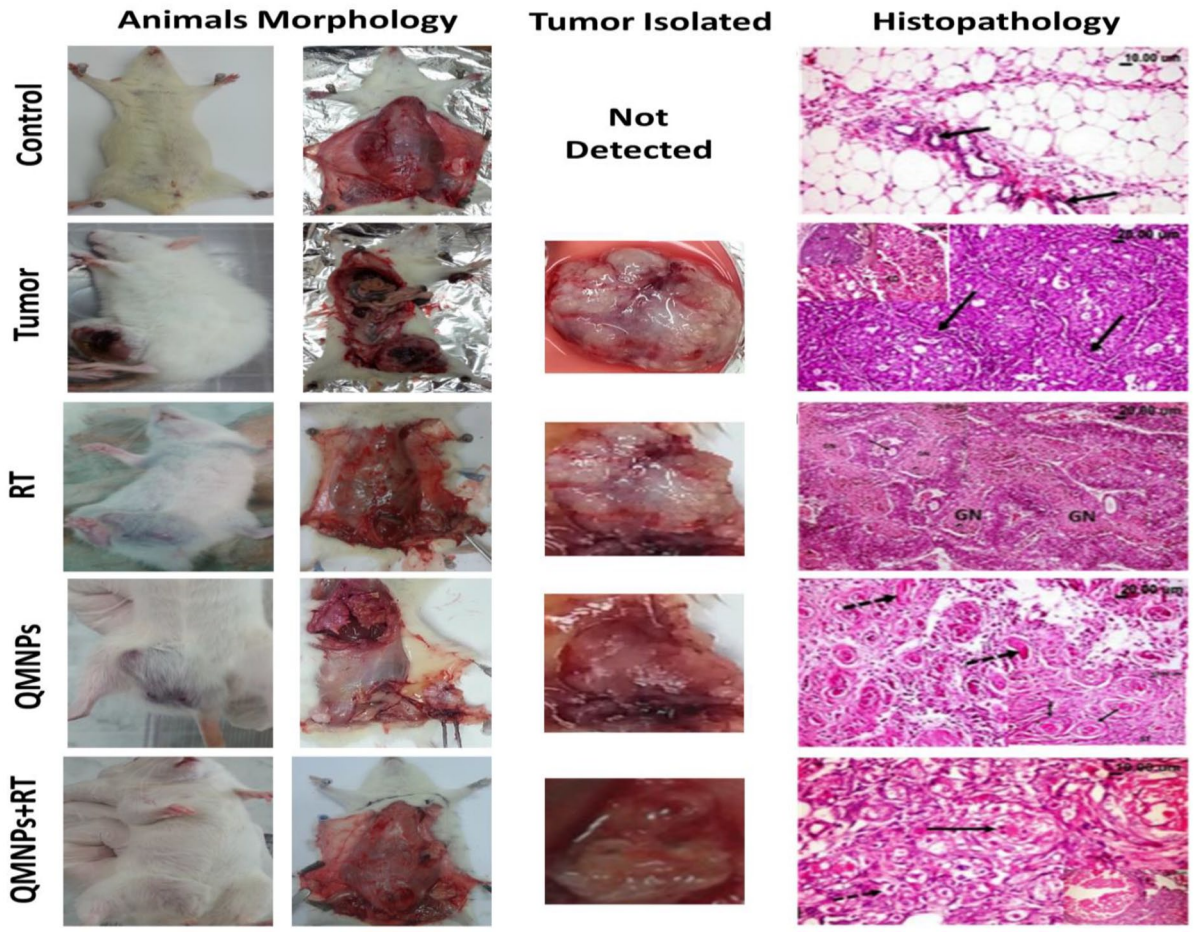

Figure 5. QMNPs and/or RT effect on morphological and histopathological indices. (Control rat) showing normal mammary acini (arrow) embedded in the surrounding adipose tissue. (Tumor rat) showing many empty spaces (arrow) in the cribriform adenocarcinoma, the top left image is showing adenocarcinoma, notice the multiple spaces within the solid masses of the tumor some are empty and others contained pink proteinaceous secretion (arrow). (RT rat showing large eosinophilic granular areas of cancer cells' necrosis [GN] among the tumor masses.). (QMNPs rat) showing marked necrosis of the cancer cells with its transformation into hyalinized eosinophilic material (arrow) as well as many pyknotic nuclei. QMNPs + RT rat showing necrosis and beginning of fibrous bands (arrow) among the cancer cell groups. Tumor size was measured using a standard caliber, in length and width, and the tumor was weighed upon excision it of all treated and untreated tumor-bearing rats. Number of animals (5 per group).
QMNP indicates quercetin magnetite nanoparticles; RT, radiotherapy.

RT-treated rats were blocked in the S phase, with a significant decrease in the Bcl-2 level, and a significant increase in the caspase-3 level, compared with those in the tumor group. However, the treatment with QMNPs induced an arrest to a proportion of cells in the G0/1 phase, with a significant increase in the sub-G1 phase (apoptosis), a significant decrease in the Bcl-2 level, and a significant increase in the caspase-3 level compared with the tumor or RT groups. In addition, the sub-G1 phase had a significant increase compared with that in the tumor group, with a significant decrease in the Bcl-2 level, and a significant increase in the caspase-3 level, compared with those in the tumor group. The combination treatment induced a higher proportion of cells in the G0/1 and sub-G1 phases, with a highly significant decrease in the Bcl-2 level, and a highly significant increase in the caspase-3 level compared with those in the tumor, RT, and QMNPs groups.

Effect of QMNPs and/or RT on CD^{4+} and CD^{8+} expression in breast tissue. The distribution of the 2 subsets of T-cell, CD^{4+} helper T-cells (Figure 6C) and the CD^{8+} cytotoxic T-cells (Figure 6D) in the control group were $22.8 \pm 2.3\%$ and $25.7 \pm 2.1\%$, respectively. The percentage of CD^{4+} increased to $29.6 \pm 2.2\%$ and the percentage of $CD8^{+}$ decreased to 16.1 ± 1.5 % in the tumor rats. The expression of CD^{4+} was decreased insignificantly after treatment with RT, while the expression of CD^{8+} was increased insignificantly after RT treatment, compared with the tumor group. Meanwhile, a marked reduction was seen in the CD^{4+} expression after QMNPs treatment, while the percentage of the CD^{8+} population was increased significantly compared with the RT and tumor groups. Otherwise, QMNPs enhanced the effect of RT treatment as indicated by the further reduction in the percentage of CD^{4+} and increase of the percentage of CD^{8+} significantly compared with the tumor, RT, and QMNPs groups.

Discussion

Magnetic nanoparticles comprise important characteristics that make them attractive for a variety of biomedical

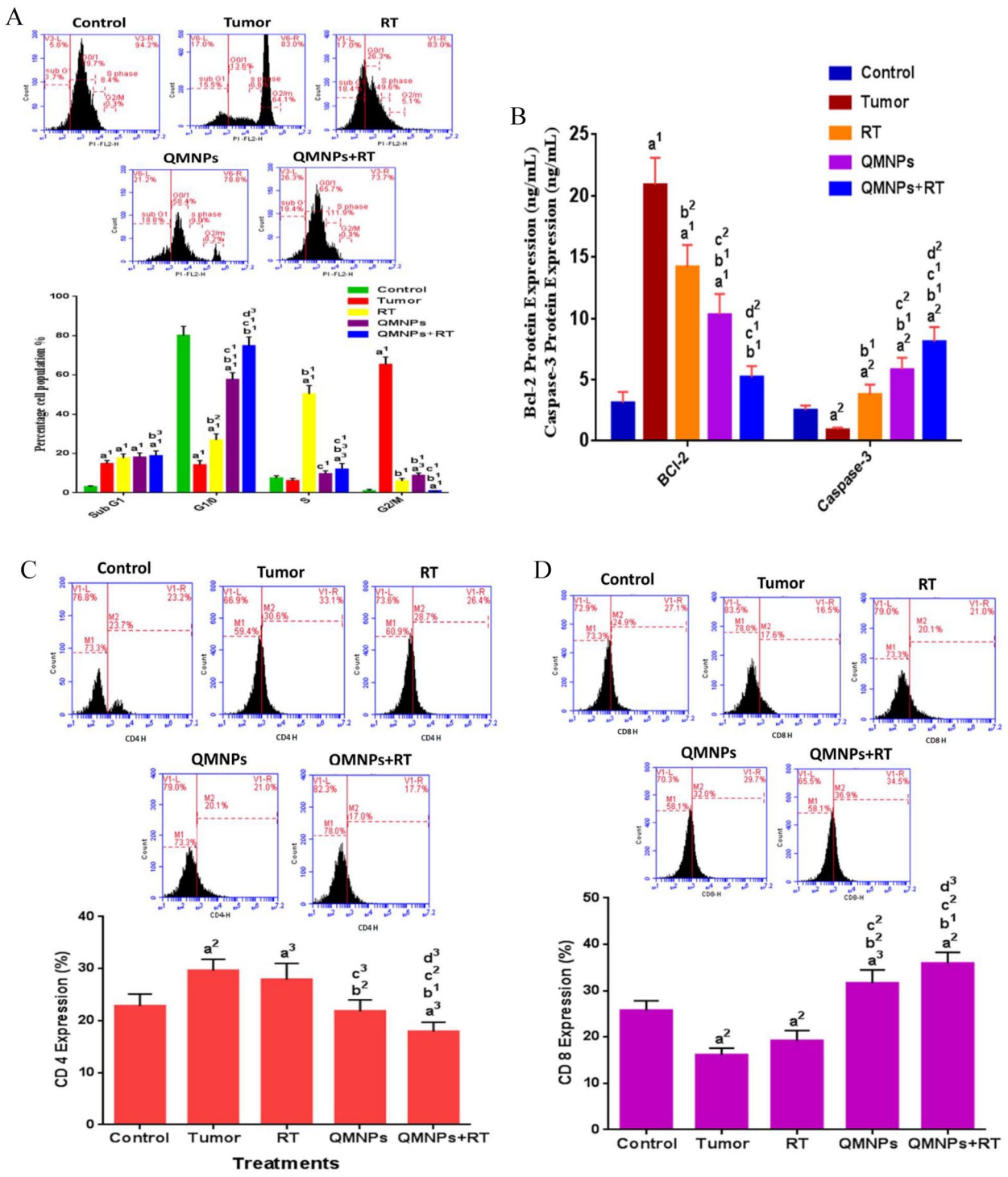

Figure 6. QMNPs and/or RT effect on cell cycle, apoptosis, CD4 and CD8: (A) cell cycle analysis, (B) Bcl-2 and caspase-3 expression, (C) CD4 expression, and (D) CD8 expression. Values expressed as the mean ± SEM, n = 5.
QMNP indicates quercetin magnetite nanoparticles; RT, radiotherapy; SEM, mean ± standard error.
$^{a1}P < .001$, $^{a2}P < .01$, $^{a3}P < .05$ vs control; $^{b1}P < .001$, $^{b2}P < .01$ vs tumor group; $^{c1}P < .001$, $^{c2}P < .01$, $^{c3}P < .05$ vs RT group; $^{d2}P < .01$, $^{d3}P < .05$ vs QMNPs group.

applications. Specifically, IONPs are physically and chemically stable, biocompatible, and environmentally safe.[20] Its effect depends on the particle size, exposure route, and exposure duration.[41] One of the advantages of NPs is used as a targeted drug delivery system to carry quercetin for chemotherapy applications.[42] To our knowledge, it is the first time to synthesize QMNPs by the eco-friendly biological method using *A. oryzae*. This was achieved by free-cell extract of *A. oryzae* and $FeSO_4$ as a substrate through a simple, cheap, and reproducible approach. The formulated substance was characterized using UV-Vis spectroscopy, TEM, XRD, and FT\IR and confirmed that Fe3O4 nanoparticles were successfully coated with quercetin. The MNPs and QMNPs were generally spherical, with an average diameter of 11 and 40 nm, respectively. Previously,

functionalization of the surface of the Fe_3O_4 nanoparticles was obtained by an electrostatic coating of quercetin onto the nanocomposite of the quercetin-Fe_3O_4 to enhance the sensitivity, specificity, stability, and reproducibility of the QMNPs.[43] Furthermore, the fabricated QMNPs exhibited dose-dependent and cell-type-specific cytotoxicity against all tested breast cancer cell lines, being MCF-7 cells were the most sensitive ones toward QMNPs with an IC_{50} value of 11.2 nm/mL. Inconsistent with our results, it has been evidenced that QFe_3O_4NPs showed concentration-dependent cytotoxicity.[44] A previous study reported that quercetin-encapsulated in solid lipid nanoparticles showed high toxicity against MCF-7 cells.[45]

The higher toxicity of QMNPs toward the breast cancer cells might be attributed to the strong binding between the MCF-7 cells and quercetin molecules due to the partial release of quercetin from the magnetite nanoparticles and magnetic oxidation that resulted in DNA damage.[22] Radiation (IR) is one of the most common modalities for breast cancer treatment; however, the outcome is limited as healthy tissues of the neighborhood of target tumor cells are adversely affected.[46] In this study, we demonstrated the optimum irradiation dose used in the subsequent *in vitro* and *in vivo* studies as adjuvant therapy in combination with QMNPs.

In this context, MCF-7 cell lines were exposed to different doses of IR (4, 6, 8, and 10 Gy) for 24 h. Our results revealed variation in a decrease of cell viability after the initial 24 h of IR exposure. The reduction in the viability was more pronounced in the MCF-7 set exposed to 6 Gy irradiation. Many *in vitro* studies have reported results from irradiation of MCF-7 cells with various doses. Some studies have indicated a decrease in the viability in MCF-cell lines exposed to 1 and 4 Gy, but the rate of the cell viability reduction by 4 Gy was slower than that of 1 Gy.[47] In agreement with our result, another group of researchers demonstrated the effect of different IR doses (1, 2, 4, 6, 8, 10, and 20 Gy) on the MCF-7. They reported that the percentage of reduction in cell viability with 6 Gy was more obvious than that of other doses.[48] The discovery of novel agents which sensitize malignant cells to the effect of radiation would increase tumor response by slowing dividing tumors sensitive to irradiation while minimizing toxicity to the surrounding organs by lowering the effective therapeutic dose.[49,50] In this regard, the role of QMNPs to enhance the radiosensitivity of MCF-7 cancer cells was evaluated. The current data of the *in vitro* study revealed that QMNPs enhanced the suppression of MCF-7 cancer cells proliferation as examined qualitatively by MTT assay and inverted light microscope, compared with the sole RT treatment alone. In the line with our findings, several studies have demonstrated the application of iron oxide nanoparticles (IONPs) as radiosensitizers.[51] In a study reported by Hauser and coworkers indicated that IONs enhanced the effect of X-ray which may be due to intensifying the production of secondary electrons and ROS and induction of DNA damage,[52] which in turn enhance radiation therapy effects by these NPs.[53] On the contrary, strong *in vitro* and *in vivo* evidence for quercetin as a radiosensitizer in tumors was reported owing to its multifunctional nature.[54] This could be due to the DNA damage effect of QMNPs owing to the magnetic oxidation via partial release of quercetin from the magnetite nanoparticles and interacts with cancer cells in an acidic environment. The cancer cells exhibit high levels of ROS, which enable them to be selectively killed by radiation. It has been demonstrated that ROS are involved in the enhancement of tumor cell radiosensitivity.[49] In this regard, our results obviously demonstrated that QMNPs either on their own or in combination with LRT enhanced the toxic effect in the tumor tissue of treated rats. This can be explained to an extent in terms of auto-oxidation of quercetin into the toxic free radicals which can irreversibly bind to various cell constituents forming sulfhydryl group and other essential groups producing secondary free radicals which are responsible for the pro-oxidant activity of quercetin.[55] Moreover, other studies reported that Fe_3O_4 acts as a radiosensitizer via enhancing the formation of ROS,[53] which could be due to the presence of pro-oxidant functional groups on their reactive surface or due to nanoparticle-cell interactions.[56] Owing to the small size of NPs and also, depending on the mode of administration and sites of deposition, these features may underlie toxicity.[57]

Regarding the acute toxicity study, the results confirmed the nontoxic nature of the synthesized QMNPs with an LD_{50} value higher than 80 mL/kg. In the subsequent *in vivo* studies, the results of hematological parameters demonstrated insignificant changes ($p > 0.05$) in ALT, AST, albumin, creatinine, urea, MDA, GSH, SOD, and CAT which could be due to its elimination from the blood circulation. One of the previous studies emphasized that IONPs introduced to the bloodstream are usually subjected to opsonization (adsorption of plasma proteins on the surface of the particles), followed by subsequent recognition and uptake by macrophages residing in the organs of the phagocytic system, ultimately resulting in the elimination from the blood circulation.[58] In addition, the *i.p.* injection is one of the main administration for IONPs which undergo hepatic metabolism before reaching the systemic circulation.[59] Liver and kidney play major roles in the metabolic transformation of drugs; hence, they are basic biosafety evaluation for drugs as well as NPs.[60] Plasma levels of liver enzyme ALT, AST activities are considered as good markers for liver toxicity.[61] The level of serum creatinine and urea concentration has been considered as useful markers for assessing nephrotoxicity.[62] Our results pointed to the non-hepatotoxic and non-nephrotoxic properties of the formulated QMNPs when used chronically in the range of the therapeutic dose. It has been reported that IONPs (γ-Fe_2O_3 and Fe_3O_4) are biocompatible, biodegradable, and non-toxic,[63] to healthy tissues.[64] Furthermore, in the toxicity study, the effect of QMNPs on lipid peroxidation and the antioxidant defense system was evaluated in plasma of treated rats compared with that of the control. Our findings

displayed a significant decrement in lipid peroxidation as indicated by the brought down of MDA level accompanied by significant elevation of GSH, SOD, and CAT. This is attributed to the increasing endogenous antioxidant levels and the free radical scavenging effect of quercetin.[65] On the contrary, other investigators demonstrated that quercetin nanoformulations attenuated the lipid peroxidation and increased antioxidant enzyme activities (SOD and CAT) and total GSH which could be due to increasing in particle bioavailability.[66]

The rodent breast cancer has been used as an experimental model for the study of mammary cancer because the mammary gland tumors of this species are similar to the most frequently diagnosed mammary cancer in women in terms of tumor histology and hormone dependence.[67] The induction of rodent mammary tumors following the administration of NMU is a widely used experimental model for investigating breast cancer in women.[68] In our *in vivo* study, the breast tumor was successfully induced experimentally in accordance with the aforementioned protocol of the current work. Induction of breast cancer recorded 100% tumor incidence (20/20) in response to *i.p.* administration of MNU carcinogen at the dose rate of 50 mg kg body weight to female albino rats at 33, 40, 47, 54, and 61 days of animal age. The same results were obtained in an early study by Russo and Russo.[69] Other investigators reported 55% tumor incidence.[70] Our observation can be explained on the basis of the susceptibility of the mammary glands to the carcinogen on the age of animals and that the high susceptibility of female rats can be observed when the carcinogen is administered during the postnatal period, between 40 to 60 days of early puberty with highly proliferating terminal end buds (TEBs) in the mammary gland.[69] In agreement to a great extent with the prior studies,[67] our results indicated that all the developed tumors were in the posterior pairs of the mammary glands of the diseased rats. The authors reported that 36/44 of the diagnosed tumors in NMU-treated rats were developed in the abdominal inguinal mammary gland. The pathological analysis demonstrated all the developed well-differentiated adenocarcinoma with various histological subtypes including solid, comedo, cribriform, and comedo cribriform subtypes and few showed cystic type. Also, there were variable degrees of ductal epithelial hyperplasia. These findings are similar to those of those who studied the histopathological alterations in the breast tissue in NMU-induced mammary tumors in female Sprague Dawley rats. Conversely, the microscopic micrographs of sections in the mammary tumors of treated rats revealed that QMNPs alone and in combination with LRT treatment showed the highest significant decrease in the tumor burden. Our results are in agreement with the study of Ren et al,[10] who found that quercetin nanoparticles inhibited liver cancer development via apoptosis induction and proliferation inhibition in the histopathology of xenograft tumors. Moreover, our histopathological observations agree with the biochemical findings which indicated that administration of QMNPs either alone or in combination with radiation therapy augmented ROS production, increased early apoptotic effect in sub G1 phase, G1/G0 cell cycle arrest, and enhancement of apoptotic effect. The changes in weight gain have often been used as sensitive indices of toxicity after exposure to toxic substances.[71] Regarding the effect of tumor incidence and different treatments on body weight gain, the current in *vivo* studies showed variations in body weight gain. In agreement with the previous observation, our results showed a significant loss in weight gain in the positive control (diseased rats) as well as LRT treatment, which might be endorsed this effect to the tumor burden.[67] Rats showed a significant gain in body weight after administration of QMNPs either alone or in combination with LRT treatment. In a study performed previously by Najafabadi et al,[17] they demonstrated the effect of superparamagnetic iron oxide nanoparticles (SPION) and quercetin superparamagnetic iron oxide nanoparticles (QT-SPION) on body weight gain in treated rats. They reported that SPION showed a significant weight loss, whereas quercetin could prevent weight loss due to the SPION. In our study, the effect of QMNPs could be attributed to the antioxidant capacity of quercetin and its ability to disclose oxidative stress. During the 28th week of the experimental period, the induction of NMU caused a great increase in the tumor burden; however, the average growth rate of tumor weight was 46.2 ± 1.3 gm and the tumor volume was found to be 739 ± 7.3 mm^3 in the diseased group, which was in agreement with the earlier report.[67] The current work revealed that both LRT treatment and QMNPs either as a sole treatment or in combination are effective in reducing the tumor burden. In the line with our results, Spiotto and Coworkers evidenced that the sole RT treatment reduces tumor burden (tumor weight and tumor volume) by inducing DNA damage.[70] Other researchers reported that quercetin-loaded chitosan nanoparticles (QCT-CS NPs) exerted a significant reduction of tumor volume after intravenous treatment of QCT-CS NPs in tumor xenograft mice in comparison to the disease group.[72] The transition from one cell cycle phase to another occurs in an orderly manner and cell cycle control is the major regulatory mechanism of cell growth.[73] So, dysregulation of the cell cycle is a key feature of cancer, and hence targeting the cell cycle is an important approach in cancer therapy.[74] In this study, our results revealed alteration of the different phases of the cell cycle in the diseased group, noting that a great reduction in cell population was observed in G1/S phases concomitant with increased cell population in the G2/M phase. The present findings are in agreement with the previously reported study, which stated that MNU caused cell cycle disturbance and increased cell population in S and G2/M phases indicating progression of cell division, meanwhile, decreased cell fractions in sub-G1.[75] Moreover, in this study, a prominent early apoptotic cell death was noticed in the sub-G1 phase and cell cycle arrest at G1 was noted upon treatment with QMNPs alone and in combination with LRT treatment indicating the

cytotoxic and radiosensitizing effect in MCF-7 cancer cells and even in tumor tissues. It has been reported that when quercetin delivered in the form of nanoparticles could induce ROS production and arrest the cell cycle in the sub-G phase in HePG2 cells,[76] increases the cells in the G1 phase of MCF-7 cells.[77] More and above, in agreement with our observations, the combination of quercetin with RT was found to enhance tumor radiosensitivity of HePG2 cells and augmented the sub-G1 population,[78] as well as in human colorectal cancer xenograft model in nude mice.[79] It is well known that the immune cells and tumor cells exert a major influence on mammary tumor development and progression.[80] In the current study, induction of mammary tumor in rats used a carcinogen (MNU) caused an obvious increase in CD^{4+} cells concomitant with a significant reduction in CD^{8+} cells in the breast tissue of diseased rats, while no significant change was observed in diseased rats received 15 Gy of LRT treatment alone, compared to the control group suggesting a negligible effect of RT on tumor-specific immune responses. Our results can be explained on the basis that CD^{8+} cell depletion decreases the therapeutic efficacy of irradiation as demonstrated in a mouse tumor model.[81] The increase of CD^{4+} and decrement in CD^{8+} in diseased untreated rats agree with Huang and coworkers who reported that CD^{4+} and CD^{8+} T-cells have opposing roles in breast cancer progression and outcomes. They concluded that CD^{8+} T-cells are the key effector cell population, mediating sufficient antitumor immunity and resulting in desirable clinical outcomes. In contrast, CD^{4+} T-cells have negative prognostic effects on breast cancer patient outcomes.[17] Regarding the immunomodulatory effect QMNPs on the immune system, the cytotoxic T-lymphocyte activity was examined via estimation of the percentage of CD^{4+} and CD^{8+} T-cells population in the breast tissue of rats. Our results revealed that QMNPs alone or in combination with LRT treatment modulated the immune response and reversed the alterations of CD^{4+} and CD^{8+}. In agreement with our observation, an earlier study performed by Oršolic et al[82] emphasized that polyphenolic compounds from *propolis* containing quercetin as one of its active components significantly increased the percentage of CD^{8+} cells and caused a reduction in the ratio between CD^{4+} and CD^{8+} lymphocytes favored to CD^{8+} in the tumor-bearing mice. The authors attributed the responses of immune activity to the immunomodulation effect and interaction of immunomodulated effectors with tumor cells. On the other hand, according to Lin et al,[79] the combination of quercetin with RT has been found to potentiate radiation-induced immunomodulation *in vitro* and *in vivo*, at least in part due to its effect on immune function. According to the literature, it seems that uptake of IONPs by T-cells was not accompanied by any measurable effects on T-cell functions.[83] The chemical induction of mammary tumor-induced carcinogenesis, a process that impairs apoptosis, which results in the development of the malignant phenotype.[84] The present study evaluated the potential therapeutic effects of QMNPs and RT administered alone and in combination on the signal transduction pathways related to apoptosis such as anti-apoptosis protein Bcl-2 and caspase-3. Our results obviously displayed increment of caspase-3 level, and downregulation Bcl-2 expression in breast tissues of diseased rats after NMU administration. It has been reported that Bcl-2 is expressed in solid tumors such as breast (about 80%), ovarian and stomach cancers.[85] In addition, earlier studies revealed that caspase-3 plays in executing apoptosis, and the observation that several examined breast cancer cells showed alteration of caspases-3 expression. Moreover, a similar loss in caspase-3 expression was evident in morphologically normal peritumoral tissue samples obtained from breast cancer patients.[86] The current observations showed that QMNPs alone and in combination with LRT treatment reversed the survival effect caused by NMU in diseased rats as indicated by increased the level of caspases-3 and brought down of Bcl-2 pointed to induction of apoptosis. In the line with our findings, a study showed quercetin resulted in downregulation of the expression of Bcl-2, Caspase-3 was also activated by quercetin, which started a caspase-3-depended mitochondrial pathway to induce apoptosis.[11] In another study, it has been elucidated that gold nanoparticles conjugated quercetin mediating cancer cell death through the caspase-3-dependent apoptosis pathway.[72] Balakrishnan et al[87] suggest that QMNPs exhibited a role in mediating antitumor and radiosensitizing by enhancing RT-induced caspase-3 activation and downregulation of antiapoptotic protein Bcl-2.

Conclusion

The results of our present investigation clearly demonstrate for the first time that QMNPs could be successfully synthesized by the green method. Quercetin-conjugated magnetite nanoparticles exhibit a striking antitumor and radio-synthetizing efficacy in MCF-7 cancer cells and in NMU animal models of breast cancer in a dose-responsive fashion (Figure 7). The antitumor and radio-synthetizing effect of QMNPs has been reflected in the ability of this compound to diminish the development of NMU-induced mammary tumors and significantly reduce tumor burden. Furthermore, our study provides considerable evidence that the breast tumor-inhibitory effect of QMNPs could be achieved, at least in part, through interference with key hallmark capabilities of tumor cells, such as abnormal cell proliferation, cell cycle arrest, immunomodulation, and induction of apoptosis. Finally, QMNPs-mediated and enhanced the LRT treatment effect on the pro-apoptotic signal during experimental induction of mammary carcinogenesis through up-regulation of pro-apoptotic proteins and downregulation of anti-apoptotic proteins of the mitochondrial apoptotic pathway. These interesting results are coupled with the safety of QMNPs as therapeutic drugs for mammary tumors.

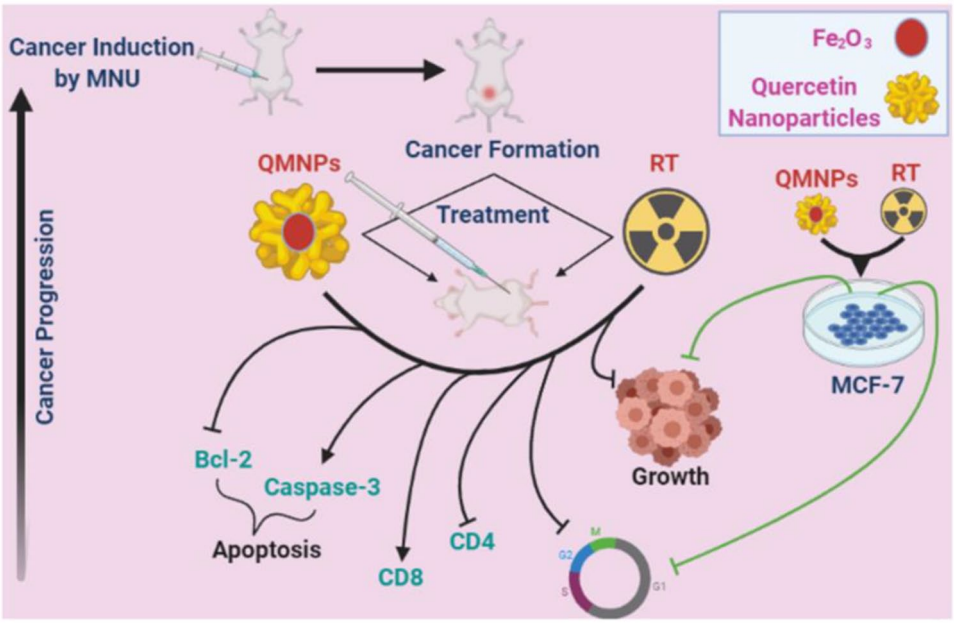

Figure 7. Summary of QMNPs and local radiotherapy (LRT) effect in breast cancer: in vitro and in vivo.
MNU indicates 1-methyl-1-nitrosourea; QMNP, quercetin magnetite nanoparticles; RT, radiotherapy.

Author Contributions

M.A.A.: experiments design, data acquisition, analysis, writing, revision, and editing. **H.A.S.E.:** data acquisition, writing, analysis, revision, and editing. **M.A.A.:** analysis, revision, and editing. **S.S.A.R.:** data analysis, data acquisition, writing, and editing. **O.E.E.**: experiments design, data acquisition, analysis, writing, revision, and editing.

Committee Approval Number

The study was approved by the research ethics committee for experimental studies (Human and Animal subjects) at NCRRT, EAEA, (Cairo, Egypt), following the 3Rs principle for animal experimentation (Replace, Reduce, and Refine) and is organized and operated according to Council for International Organizations of Medical Sciences and International Council for Laboratory Animal Science International Guiding Principles for Biomedical Research Involving Animals 2012 (serial number: 4A/20).

Data Availability Statement

All data generated or analyzed during this study are included in this manuscript.

ORCID iD

Mostafa A Askar https://orcid.org/0000-0003-3967-2018

REFERENCES

1. Riggio AI, Varley KE, Welm AL. The lingering mysteries of metastatic recurrence in breast cancer. *Br J Cancer*. 2021;124:13-26.
2. Siegel RL, Miller KD, Jemal A. Cancer statistics, 2020. *CA Cancer J Clin*. 2020;70:7-30.
3. Sherman JH, Kirzner J, Siu A, Amos S, Hussaini IM. Sorafenib tosylate as a radiosensitizer in malignant astrocytoma. *J Clin Neurosci*. 2014;21:131-136.
4. Baskar R, Dai J, Wenlong N, Yeo R, Yeoh KW. Biological response of cancer cells to radiation treatment. *Front Mol Biosci*. 2014;1:24.
5. Ray PD, Huang BW, Tsuji Y. Reactive oxygen species (ROS) homeostasis and redox regulation in cellular signaling. *Cell Signal*. 2012;24:981-990.
6. Agoni L, Basu I, Gupta S, et al. Rigosertib is a more effective radiosensitizer than cisplatin in concurrent chemoradiation treatment of cervical carcinoma, in vitro and in vivo. *Int J Radiat Oncol Biol Phys*. 2014;88:1180-1187.
7. Mitra S, Dash R. Natural products for the management and prevention of breast cancer. *Evid Based Complement Alternat Med*. 2018;2018:8324696.
8. Abdelghffar EA, El-Nashar HAS, Al-Mohammadi AGA, Eldahshan OA. Orange fruit (*Citrus sinensis*) peel extract attenuates chemotherapy-induced toxicity in male rats. *Food Funct*. 2021;12:9443-9455.
9. El-Nashar HAS, Eldahshan OA, Elshawi OE, Singab ANB. Phytochemical investigation, antitumor activity, and hepatoprotective effects of acrocarpus fraxinifolius leaf extract. *Drug Dev Res*. 2017;78:210-226.
10. Ren KW, Li YH, Wu G, et al. Quercetin nanoparticles display antitumor activity via proliferation inhibition and apoptosis induction in liver cancer cells. *Int J Oncol*. 2017;50:1299-1311.
11. Niu G, Yin S, Xie S, et al. Quercetin induces apoptosis by activating caspase-3 and regulating Bcl-2 and cyclooxygenase-2 pathways in human HL-60 cells. *Acta Biochim Biophys Sin (Shanghai)*. 2011;43:30-37.
12. Huang Y, Ma C, Zhang Q, et al. CD4+ and CD8+ T cells have opposing roles in breast cancer progression and outcome. *Oncotarget*. 2015;6:17462-17478.
13. Whiteside TL. Immune responses to cancer: are they potential biomarkers of prognosis? *Front Oncol*. 2013;3:107.
14. Tungmunnithum D, Thongboonyou A, Pholboon A, Yangsabai A. Flavonoids and other phenolic compounds from medicinal plants for pharmaceutical and medical aspects: an overview. *Medicines (Basel, Switzerland)*. 2018;5:93.
15. Gun SY, Lee SWL, Sieow JL, Wong SC. Targeting immune cells for cancer therapy. *Redox Biol*. 2019;25:101174.
16. Brito AF, Ribeiro M, Abrantes AM, et al. Quercetin in cancer treatment, alone or in combination with conventional therapeutics? *Curr Med Chem*. 2015;22:3025-3039.
17. Najafabadi RE, Kazemipour N, Esmaeili A, Beheshti S, Nazifi S. Quercetin prevents body weight loss due to the using of superparamagnetic iron oxide nanoparticles in rat. *Adv Biomed Res*. 2018;7:8.
18. Amanzadeh E, Esmaeili A, Abadi REN, Kazemipour N, Pahlevanneshan Z, Beheshti S. Quercetin conjugated with superparamagnetic iron oxide nanoparticles improves learning and memory better than free quercetin via interacting with proteins involved in LTP. *Sci Rep*. 2019;9:6876.
19. Li C, Zhang J, Zu YJ, et al. Biocompatible and biodegradable nanoparticles for enhancement of anti-cancer activities of phytochemicals. *Chin J Nat Med*. 2015;13:641-652.
20. Arias LS, Pessan JP, Vieira APM, Lima TMT, Delbem ACB, Monteiro DR. Iron oxide nanoparticles for biomedical applications: a perspective on synthesis, drugs, antimicrobial activity, and toxicity. *Antibiotics (Basel, Switzerland)*. 2018;7:46.

21. Fatemi M, Mollania N, Momeni-Moghaddam M, Sadeghifar F. Extracellular biosynthesis of magnetic iron oxide nanoparticles by Bacillus cereus strain HMH1: characterization and in vitro cytotoxicity analysis on MCF-7 and 3T3 cell lines. *J Biotechnol*. 2018;270:1-11.
22. Siddiqi KS, Husen A. Fabrication of metal nanoparticles from fungi and metal salts: scope and application. *Nanoscale Res Lett*. 2016;11:98.
23. Mekawey AA, Helmy EA. Elucidative physiological optimization of silver nanospheres biogenesis by molds. *Int J Nanotechnol Allied Sci*. 2017;1:30-44.
24. Dey S, Spring PM, Arnold S, et al. Low-dose fractionated radiation potentiates the effects of Paclitaxel in wild-type and mutant p53 head and neck tumor cell lines. *Clin Cancer Res*. 2003;9:1557-1565.
25. ISO/ASTM 51026:2015. Practice for using the Fricke dosimeter system.
26. Liao YP, Wang CC, Schaue D, Iwamoto KS, McBride WH. Local irradiation of murine melanoma affects the development of tumour-specific immunity. *Immunology*. 2009;128:e797-e804.
27. Gupta A, Probst HC, Vuong V, et al. Radiotherapy promotes tumor-specific effector CD8+ T cells via dendritic cell activation. *J Immunol (Baltimore, MD)*. 2012;189:558-566.
28. Foo JB, Yazan LS, Tor YS, et al. Induction of cell cycle arrest and apoptosis in caspase-3 deficient MCF-7 cells by Dillenia suffruticosa root extract via multiple signalling pathways. *BMC Complement Altern Med*. 2014;14:197.
29. Liska J, Galbavy S, Macejova D, Zlatos J, Brtko J. Histopathology of mammary tumours in female rats treated with 1-methyl-1-nitrosourea. *Endocr Regul*. 2000;34:91-96.
30. Shibata MA, Morimoto J, Shibata E, et al. Raloxifene inhibits tumor growth and lymph node metastasis in a xenograft model of metastatic mammary cancer. *BMC Cancer*. 2010;10:566.
31. Reitman S, Frankel S. A colorimetric method for the determination of serum glutamic oxalacetic and glutamic pyruvic transaminases. *Am J Clin Pathol*. 1957;28:56-63.
32. Tietz NW, Pruden EL, Fuhrman SA. *Clinical Guide to Laboratory Tests*. Philadelphia, PA: WB Saunders; 1995.
33. Di Giorgio J, Henry R, Winkelman J. Nonprotein nitrogenous constituents. In: Henry R, Canon D, Winkelman J, eds. *Clinical Chemistry Principles and Techniques*. New York, NY: Harper & Row; 1974:870.
34. Shephard MD, Mazzachi RD. Scientific and Technical Committee: technical report no. 8. The collection, preservation, storage and stability of urine specimens for routine clinical biochemical analysis. *Clin Biochem Rev*. 1983;4:61-67.
35. Yoshioka T, Kawada K, Shimada T, Mori M. Lipid peroxidation in maternal and cord blood and protective mechanism against activated-oxygen toxicity in the blood. *Am J Obstet Gynecol*. 1979;135:372-376.
36. Beutler E, Duron O, Kelly BM. Improved method for the determination of blood glutathione. *J Lab Clin Med*. 1963;61:882-888.
37. Minami M, Yoshikawa H. A simplified assay method of superoxide dismutase activity for clinical use. *Clin Chim Acta*. 1979;92:337-342.
38. Sinha AK. Colorimetric assay of catalase. *Anal Biochem*. 1972;47:389-394.
39. Bancroft JD, Gamble M. *Theory and Practice of Histological Techniques*. Philadelphia, PA: Elsevier Health Sciences; 2008.
40. Heinlein C, Deppert W, Braithwaite A, Speidel D. A rapid and optimization-free procedure allows the in vivo detection of subtle cell cycle and ploidy alterations in tissues by flow cytometry. *Cell Cycle*. 2010;9:3584-3590.
41. Ansari SAMK, Ficiarà E, Ruffinatti FA, Stura I, et al. Magnetic iron oxide nanoparticles: synthesis, characterization and functionalization for biomedical applications in the central nervous system. *Materials*. 2019;12:465.
42. Akal Z, Alpsoy L, Baykal A. Superparamagnetic iron oxide conjugated with folic acid and carboxylated quercetin for chemotherapy applications. *Ceram Int*. 2016;42:9065-9072.
43. Wang Z. Iron complex nanoparticles synthesized by Eucalyptus leaves. *ACS Sustain Chem Eng*. 2013;1:1551-1554.
44. Laurent S, Mahmoudi M. Superparamagnetic iron oxide nanoparticles: promises for diagnosis and treatment of cancer. *Int J Mol Epidemiol Genet*. 2011;2:367-390.
45. Niazvand F, Orazizadeh M, Khorsandi L, Abbaspour M, Mansouri E, Khodadadi A. Effects of quercetin-loaded nanoparticles on MCF-7 human breast cancer cells. *Medicina (Kaunas, Lithuania)*. 2019;55:114.
46. Rezvani M. Amelioration of the pathological changes induced by radiotherapy in normal tissues. *J Pharm Pharmacol*. 2008;60:1037-1048.
47. Bartelink H, Horiot JC, Poortmans PM, et al. Impact of a higher radiation dose on local control and survival in breast-conserving therapy of early breast cancer: 10-year results of the randomized boost versus no boost EORTC 22881-10882 trial. *J Clin Oncol*. 2007;25:3259-3265.
48. Wang Y-l, Zhang H, Li N, Wang X-h, Hao J-f, Zhao W-p. Potential mechanisms involved in resistant phenotype of MCF-7 breast carcinoma cells to ionizing radiation induced apoptosis. *Nucl Instrum Methods Phys Res B*. 2009;267:1001-1006.
49. Kermanian M, Naghibi M, Sadighian S. One-pot hydrothermal synthesis of a magnetic hydroxyapatite nanocomposite for MR imaging and pH-Sensitive drug delivery applications. *Heliyon*. 2020;6:e04928. doi:10.1016/j.heliyon.2020.e04928.
50. Moding EJ, Kastan MB, Kirsch DG. Strategies for optimizing the response of cancer and normal tissues to radiation. *Nat Rev Drug Discov*. 2013;12:526-542.
51. Liu Y, Zhang P, Li F, et al. Metal-based nanoenhancers for future radiotherapy: radiosensitizing and synergistic effects on tumor cells. *Theranostics*. 2018;8:1824-1849.
52. Hauser AK, Mitov MI, Daley EF, McGarry RC, Anderson KW, Hilt JZ. Targeted iron oxide nanoparticles for the enhancement of radiation therapy. *Biomaterials*. 2016;105:127-135.
53. Retif P, Pinel S, Toussaint M, et al. Nanoparticles for radiation therapy enhancement: the key parameters. *Theranostics*. 2015;5:1030-1044.
54. Gong C, Yang Z, Zhang L, Wang Y, Gong W, Liu Y. Quercetin suppresses DNA double-strand break repair and enhances the radiosensitivity of human ovarian cancer cells via p53-dependent endoplasmic reticulum stress pathway. *Onco Targets Ther*. 2018;11:17-27.
55. Geetha T, Malhotra V, Chopra K, Kaur IP. Antimutagenic and antioxidant/prooxidant activity of quercetin. *Indian J Exp Biol*. 2005;43:61-67.
56. Sarkar A, Ghosh M, Sil PC. Nanotoxicity: oxidative stress mediated toxicity of metal and metal oxide nanoparticles. *J Nanosci Nanotechnol*. 2014;14:730-743.
57. Yildirimer L, Thanh NT, Loizidou M, Seifalian AM. Toxicology and clinical potential of nanoparticles. *Nano Today*. 2011;6:585-607.
58. Gustafson HH, Holt-Casper D, Grainger DW, Ghandehari H. Nanoparticle uptake: the phagocyte problem. *Nano Today*. 2015;10:487-510.
59. Turner PV, Brabb T, Pekow C, Vasbinder MA. Administration of substances to laboratory animals: routes of administration and factors to consider. *J Am Assoc Lab Anim Sci*. 2011;50:600-613.
60. Yang Y, Qin Z, Zeng W, et al. Toxicity assessment of nanoparticles in various systems and organs. *Nanotechnol Rev*. 2017;6:279-289.
61. Atici S, Cinel I, Cinel L, Doruk N, Eskandari G, Oral U. Liver and kidney toxicity in chronic use of opioids: an experimental long term treatment model. *J Biosci*. 2005;30:245-252.
62. Gowda S, Desai PB, Kulkarni SS, Hull VV, Math AA, Vernekar SN. Markers of renal function tests. *N Am J Med Sci*. 2010;2:170-173.
63. Estelrich J, Escribano E, Queralt J, Busquets MA. Iron oxide nanoparticles for magnetically-guided and magnetically-responsive drug delivery. *Int J Mol Sci*. 2015;16:8070-8101.
64. Wadajkar AS, Menon JU, Kadapure T, Tran RT, Yang J, Nguyen KT. Design and application of magnetic-based theranostic nanoparticle systems. *Recent Pat Biomed Eng*. 2013;6:47-57.
65. Kalantari H, Foruozandeh H, Khodayar MJ, Siahpoosh A, Saki N, Kheradmand P. Antioxidant and hepatoprotective effects of Capparis spinosa L. fractions and quercetin on tert-butyl hydroperoxide-induced acute liver damage in mice. *J Tradit Complement Med*. 2018;8:120-127.
66. Ghaffari F, Hajizadeh Moghaddam A, Zare M. Neuroprotective effect of quercetin nanocrystal in a 6-hydroxydopamine model of Parkinson disease: biochemical and behavioral evidence. *Basic Clin Neurosci*. 2018;9:317-324.
67. Saminathan M, Rai R, Dhama K, et al. Histopathology and immunohistochemical expression of N-methyl-N-nitrosourea (NMU) induced mammary tumours in Sprague-Dawley rats. *Asian J Anim Vet Adv*. 2014;9:621-640.
68. Chan MM, Lu X, Merchant FM, Iglehart JD, Miron PL. Gene expression profiling of NMU-induced rat mammary tumors: cross species comparison with human breast cancer. *Carcinogenesis*. 2005;26:1343-1353.
69. Russo IH, Russo J. Mammary gland neoplasia in long-term rodent studies. *Environ Health Perspect*. 1996;104:938-967.
70. Spiotto M, Fu YX, Weichselbaum RR. The intersection of radiotherapy and immunotherapy: mechanisms and clinical implications. *Sci Immunol*. 2016;1:EAAG1266.
71. Vaghasiya Y, Shukla V, Chanda S. Acute oral toxicity study of Pluchea arguta boiss extract in mice. *J Pharmacol Toxicol*. 2011;6:113-123.
72. Baksi R, Singh DP, Borse SP, Rana R, Sharma V, Nivsarkar M. In vitro and in vivo anticancer efficacy potential of quercetin loaded polymeric nanoparticles. *Biomed Pharmacother*. 2018;106:1513-1526.
73. Otto T, Sicinski P. Cell cycle proteins as promising targets in cancer therapy. *Nat Rev Cancer*. 2017;17:93-115.
74. Fu Y, Kadioglu O, Wiench B, et al. Cell cycle arrest and induction of apoptosis by cajanin stilbene acid from Cajanus cajan in breast cancer cells. *Phytomedicine*. 2015;22:462-468.
75. Xu B, Kim S, Kastan MB. Involvement of Brca1 in S-phase and G(2)-phase checkpoints after ionizing irradiation. *Mol Cell Biol*. 2001;21:3445-3450.

76. Bishayee K, Khuda-Bukhsh AR, Huh SO. PLGA-loaded gold-nanoparticles precipitated with quercetin downregulate HDAC-Akt activities controlling proliferation and activate p53-ROS crosstalk to induce apoptosis in hepatocarcinoma cells. *Mol Cells*. 2015;38:518-527.
77. Ranganathan S, Halagowder D, Sivasithambaram ND. Quercetin suppresses twist to induce apoptosis in MCF-7 breast cancer cells. *PLoS ONE*. 2015;10:e0141370.
78. Jang J, Kang M, Lim Y, Kim J, Kim J. Effects of quercetin on ionizing radiation-induced cellular responses in HepG2 cells. *Int J Radiat Res*. 2017;15:229-239.
79. Lin C, Yu Y, Zhao H-g, Yang A, Yan H, Cui Y. Combination of quercetin with radiotherapy enhances tumor radiosensitivity in vitro and in vivo. *Radiother Oncol*. 2012;104:395-400.
80. Gu-Trantien C, Loi S, Garaud S, et al. CD4' follicular helper T cell infiltration predicts breast cancer survival. *J Clin Invest*. 2013;123:2873-2892.
81. Takeshima T, Chamoto K, Wakita D, et al. Local radiation therapy inhibits tumor growth through the generation of tumor-specific CTL: its potentiation by combination with Th1 cell therapy. *Cancer Res*. 2010;70:2697-2706.
82. Oršolic N, Terzic S, Šver L, Bašic I. Polyphenolic compounds from propolis modulate immune responses and increase host resistance to tumour cells. *Food Agric Immunol*. 2005;16:165-179.
83. Shah A, Dobrovolskaia MA. Immunological effects of iron oxide nanoparticles and iron-based complex drug formulations: therapeutic benefits, toxicity, mechanistic insights, and translational considerations. *Nanomedicine*. 2018;14:977-990.
84. Rocak SG, Karabulut AB, Tuzcu M, et al. Combinatorial effect of zoledronic acid and irradiation on the prevention of DMBA-induced precancerogenic changes in the mammary tissues of rats. *J Cancer Res Ther*. 2016;12:645-649.
85. Bouchalova K, Kharaishvili G, Bouchal J, Vrbkova J, Megova M, Hlobilkova A. Triple negative breast cancer—BCL2 in prognosis and prediction. *Curr Drug Targets*. 2014;15:1166-1175.
86. Devarajan E, Sahin AA, Chen JS, et al. Down-regulation of caspase 3 in breast cancer: a possible mechanism for chemoresistance. *Oncogene*. 2002;21:8843-8851.
87. Balakrishnan S, Mukherjee S, Das S, et al. Gold nanoparticles-conjugated quercetin induces apoptosis via inhibition of EGFR/PI3K/Akt-mediated pathway in breast cancer cell lines (MCF-7 and MDA-MB-231). *Cell Biochem Funct*. 2017;35:217-231.